Undulating Topography of HfO_2 Thin Films Deposited in a Mesoscale Reactor Using Hafnium (IV) *tert* Butoxide

Kejing Li
Chemical and Biological Engineering Dept, The University of Alabama, Tuscaloosa, AL 35487

Lin Zhang
Center for Composite Materials and Structures, Harbin Institute of Technology, Harbin 150001, People's Republic of China

David A. Dixon
Chemistry Dept, The University of Alabama, Tuscaloosa, AL 35487

Tonya M. Klein
Chemical and Biological Engineering Dept, The University of Alabama, Tuscaloosa, AL 35487

DOI 10.1002/aic.12504
Published online February 16, 2011 in Wiley Online Library (wileyonlinelibrary.com).

HfO_2 was deposited by chemical vapor deposition on Si, native SiO_2, and borosilicate glass surfaces using hafnium (IV) tert *butoxide in a mesoscale flow reactor. Undulating thin film topographies were observed by atomic force microscopy on all substrates with peak-to-peak periods between 10 and 25 nm in the presence of a temperature gradient perpendicular to flow of 25°C/mm. A computational fluid dynamic model suggests the phenomenon originates from buoyancy driven roll type flow. The thickness uniformity and roughness of the films depended on the flow rate, reactor temperature, and the substrate type.* © 2011 American Institute of Chemical Engineers *AIChE J,* 57: 2989–2996, 2011
Keywords: adsorption/gas, computational fluid dynamics, chemical vapor deposition, thin film, heat transfer

Introduction

Chemical vapor deposition (CVD) is an important technique in thin film deposition and is widely applied in thin film layers or coatings for microelectronic devices, microelectro-mechanical systems, hard drive read/write heads, anticorrosion layers, and other related technologies.[1] In most cases, a film with atomic scale composition uniformity and topographic conformality is desired and is determined by the precursor, mass transport, flow dynamics, temperature uniformity, and reaction kinetics.[2,3] In low pressure CVD reactors, the flow is typically laminar because of the fluid density, reactor dimension, and velocity. For smaller reactor dimensions such as those approaching the boundary layer thickness, a closer examination of the shear force near the wall is required. These velocity fields can determine the local evolution of hillocks, which may be useful for specialized applications such as friction coatings or patterned media.

Among common production reactors, the horizontal type reactor is the main production tool for growing polycrystalline Si, dielectric materials, and passivating films used in Si integrated-circuit manufacturing.[4] During the deposition, the precursor is fed perpendicular to the gravitational field. Chemical reaction engineering, flow behavior, and mass transfer have significant impacts on CVD.[5,6] The depletion

Additional Supporting Information may be found in the online version of this article.

Correspondence concerning this article should be addressed to T. M. Klein at tklein@eng.ua.edu.

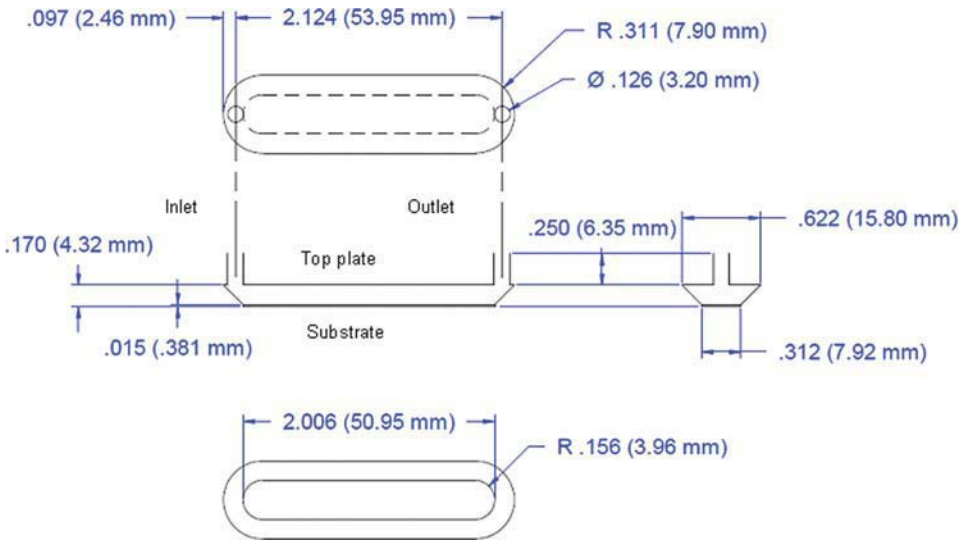

Figure 1. Schematic drawing of the inside of the flow-through cell with dimensions (by permission from Harrick Scientific Products, Inc.)

The dimensions of the substrate are shown at the bottom of the diagram. [Color figure can be viewed in the online issue, which is available at wileyonlinelibrary.com.]

of reactants downstream and free convection due to temperature differences between the substrate and the wall[7] have been shown to cause thin film nonuniformity in horizontal reactors. The purpose of the this work is to obtain some understanding of the fluid behavior in a horizontal type mesoscale CVD reactor to explain the formation of observed periodic undulations on the order of 10–25 nm.

Because of the complexity in a CVD reactor, how the precursor vapor transport influences the film growth kinetic behavior has been modeled[7] but relatively few supporting experiments directly addressing this issue have been performed. HfO_2 is a high dielectric metal oxide that can be used in metal oxide semiconductor field effect transistors. CVD of HfO_2 growth from hafnium *tert*-butoxide (HTB) has been reported.[8] In our previous work,[9] the mechanism for HTB adsorption and reaction on semiconductor surfaces were studied. In this article, a fluid dynamic effect on thin film growth is addressed.

Experimental Methods

The flow-through CVD reaction system setup is described elsewhere.[9] The Hf precursor HTB (99.99% purity from Strem Chemicals, Inc.) was transferred to a quartz bubbler under N_2 and heated in an oil bath at temperatures between 50–75°C (vapor pressure 9.3 Pa at 25°C and 133.3 Pa at 65°C). The reactor size is a 100 × 50 × 8 mm on the inside and its dimensions are given in Figure 1.

The reactor body is bigger than micro reactors at the millimeter scale[10] but smaller than industrial CVD flow reactors. It is made of stainless steel (ss), with inlet and outlet tubes designed to be compatible to vacuum fittings. The substrate is fixed and changeable at the bottom plate. The reactor is heated by a top smaller rectangular plate embodying two copper heating rods (The dimensions and schematic drawing of the meso reactor is given in Supporting Information, Figure S1). The setting temperature (ST) is monitored by a thermocouple inside the top heating plate. With increasing ST, the temperature difference between the top plate and the substrate increases to about 100°C at ST = 250°C (see Figures S2 and S3 in the Supporting Information for finite element analysis heat transfer models and experimental temperature measurements). The direction along the substrate is defined as the X axis. Three substrate materials were used: n-type 0.01 parts per million boron doped Si (100) wafers treated with 1:1:100 $HF:NH_4F:H_2O$ buffered oxide etch; 1.0 nm native silicon oxide; and borax glass. All three materials are atomically flat, with RMS roughness less than several angstroms, as shown in Figure 2, for example.

The substrates were pressed to the bottom ss body by one sheet of ss cover and two aluminum covers, and the substrate was sealed to the ss body by a Kalrez® gasket. HTB and the bubbler were kept in an oil bath with controllable

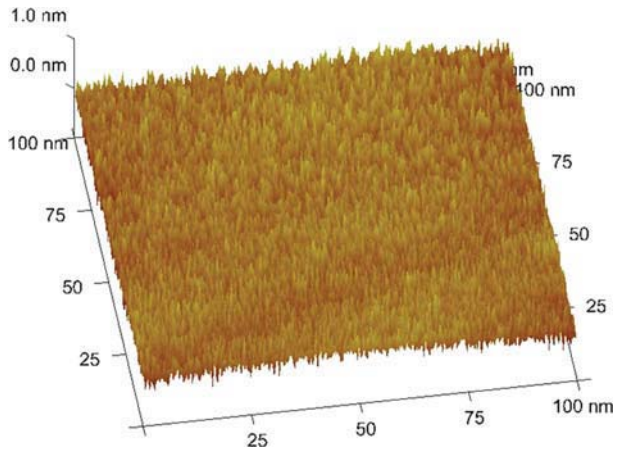

Figure 2. Atomically flat substrates.

As an example, the BOE treated H-Si(100) substrate. [Color figure can be viewed in the online issue, which is available at wileyonlinelibrary.com.]

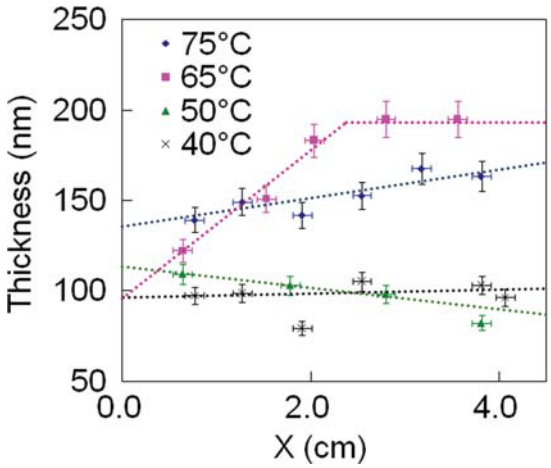

Figure 3. Thickness of HfO_2 along axis on Si wafer with different bubbler temperatures and a ST temperature of 250°C.

Lines are drawn only to guide the eye. [Color figure can be viewed in the online issue, which is available at wileyonlinelibrary.com.]

temperatures. The bubbler was preheated and stabilized for 45 min before introducing the precursor to the flow cell. The base absolute pressure reading was 0.13 Pa for a downstream Pirani pressure gauge, and the experimental pressure was around 40 Pa depending on the bubbler and reactor temperature. No carrier gas was used due to the high vapor pressure of HTB. A bypass line of Ar was used to calibrate the flow rate and purge the gas line before and after each experiment.

After a deposition time of 1 h, the cell was cooled down and the brittle substrate was carefully removed for thin film property measurements. The thickness was measured with an interferometer (F20 by Filmetrics, Inc.). Roughness and morphology were measured by an atomic force microscope (AFM) using an ultrasharp silicon cantilever NSC14/AIBS of 10-nm tip radius (Mikro Masch, Narva) with a force constant of $\sim$ 5.7 N/m and a resonant frequency of about $\sim$ 160 kHz on a Digital Instruments Dimension 3100 Scans Probe Microscope with NanoScope VI controller.

Experimental Results

Thickness measurements

The film thickness is a function of deposition time and deposition rate. Instead of growing ultrathin films, we focus on the fluid behavior during the deposition. Films with thicknesses more than 100 nm were grown at temperatures between 200°C (onset of deposition) and 300°C (limit of the Kalrez® gasket) for 1 h at a deposition rate of 0.8–3.3 nm/min. Figure 3 shows the thickness variation along the axis after 1 h of deposition with different bubbler temperatures when the ST was 250°C. On average, the higher the bubbler temperature, the faster the growth rate due to a higher vapor pressure.

Assuming several factors remain consistent along the axis including chemical composition, starting surface, coverage, and residence time, the growth kinetics is a function of temperature and concentration. It was noted that in horizontal reactors, depletion occurs along the streamline due to a smaller partial pressure downstream (see discussion of pressure in the Supporting Information). Figure 3 shows that by changing the bubbler temperature, the precursor can either accumulate or be depleted at the latter part of the substrate, depending on the supply of precursors. For 65°C, there are many possible causes for the accumulation. As the top plate is hotter than the bottom substrate and possibly has a lower trapping coefficient on the ss, it is possible that there are gaseous intermediates which may physisorb and desorb a number of times before sticking to a surface site. Because of a longer residence time in the horizontal reactor at the back end, the reactive intermediate concentration is higher than at the front end. Variation in the velocity field across the reactor can lead to film thickness dispersion. For lower bubbler temperatures at 50 and 40°C (lower vapor thickness), the thickness decrease along the axis is a reflection of the decrease of the number of molecules per unit volume or the reactant concentration. The dip in the thickness at X $\sim$ 2 cm at 40°C could rise from the depletion of the precursors due to rolls or eddies at the front end of the substrate. However, for an even higher vapor supply such as a bubbler temperature of 75°C, the higher pressure is compensated by the effect of increased surface diffusivity, which results in a more uniform film.

Figure 4 shows the axial thickness variation on native silicon oxide for various heating plate ST with a bubbler temperature of 65°C. The reaction becomes mass transfer limited at 300°C, and depletion caused a thickness decrease to occur along the axis. We note that special attention has to be paid to sample preparation and the time between disassembly and sample removed for the thickness measurement (see Supporting Information Figure S4).

Even without knowing the detailed reaction mechanism and composition uniformity, the thickness can be modulated by adjusting the flux and substrate temperature. However, a complex flow pattern may exist that makes achieving uniform films nontrivial. Mixed convection may affect the thin film growth by the concentration of vapor supply and on the density of films. The formed topography of thin films in a CVD horizontal reactor with a uniform substrate temperature profile can

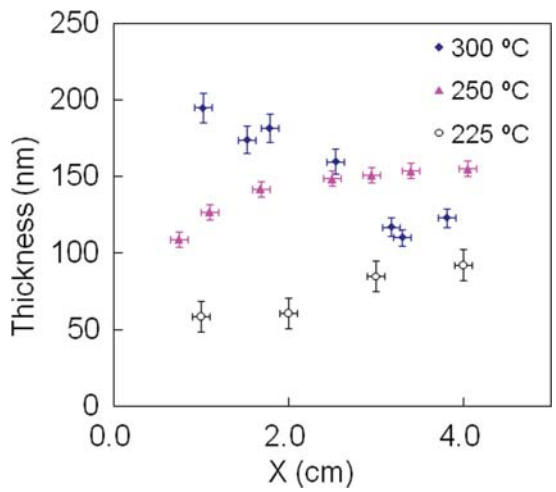

Figure 4. Thickness along axis on the native oxide with different heating plate ST, 1 h of HTB adsorption with bubbler temperature of 65°C.

[Color figure can be viewed in the online issue, which is available at wileyonlinelibrary.com.]

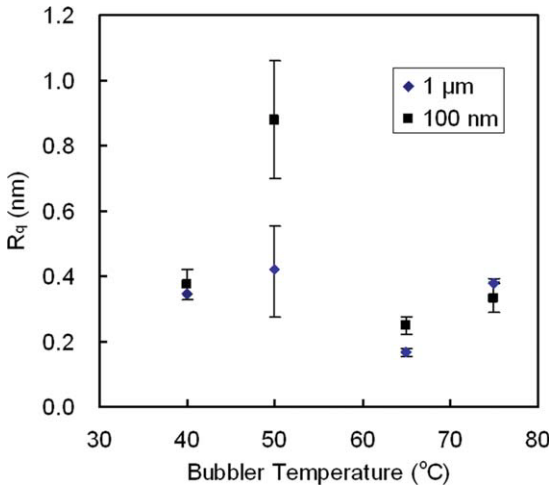

Figure 5. Roughness of HfO_2 thin films at $X = 3$ cm on native oxide with different bubbler temperatures with ST at 250°C.

The two series represent different AFM scan areas. [Color figure can be viewed in the online issue, which is available at wileyonlinelibrary.com.]

reflect the gas phase flow supply by a degree as discussed in the following section. The quantitative analysis of transverse dispersion in a particular flow has to be analyzed by precise calculations which require careful setting of the parameters.

Roughness measurements

Starting with different surfaces, the final HfO_2 thin film roughness behaves differently. On average, with an H-Si surface, the HfO_2 thin film roughness decreased with an increase in the thickness, whereas for a native oxide on a Si wafer, the thin film roughness increased with an increase in the thickness. The average roughness for 1 h of HTB deposition along the axis at 250°C on a native oxide at X ~ 3 cm is shown in Figure 5 for four bubbler temperatures. The roughness is the highest for the bubbler temperature of 50°C for both the 1 μm and 100 nm scales, and these values have the largest error bars as well. There is not much difference between the two length scales for the other three bubbler temperatures. The vapor pressure is 13.3, 53.3, 133.3, and 440.0 Pa at temperatures of 40, 50, 65, and 75°C, respectively, based on the Clapeyron equation and reported data.[11,12] The enhancement at 50°C could be due to the increased vapor pressure of the HTB leading to a change in the flow of the gas due to a higher gas density and decreased diffusivity and a substantial change in the CVD process. As the temperature is increased, other reactivity effects can also become more important, which reduce the change in the roughness. This is discussed in more detail below.

During the deposition experiment, the pressure was around 40.0 Pa. As the Si substrate temperature was set at 250°C, the ratio of the substrate temperature to the HfO_2 melting point 2812°C is about 0.17, and minimal adatom diffusion is expected. Thus, the film has many defects, is fine grained, has a columnar structure, and has low density boundaries between columns based on the Movchan–Demchishin model.[2] In this case, any roughness is actually very small compared to the film thickness.

AFM images

Figure 6 shows the AFM image of the film deposited on native oxide with varying bubbler temperatures at a ST temperature of 250°C. Different patterns occur for different flow fluxes. The larger roughness at 50°C required that the height shown be doubled. Figure 7 is a similar experiment using three different surfaces: H-Si(100) treated with buffered hydrofluoric acid; an n-Si(100) wafer with a 1.0 nm native oxide surface; and Borax glass. All reactor STs were 250°C. The bubbler temperature was 65°C for the H-Si(100), 50°C for the native Si oxide surfaces, and 50°C for the Borax glass. Stripes perpendicular to the axis or flow direction with a periodicity of 10–25 nm were observed on all the three substrates under appropriate conditions. It is likely that higher flow rates produced buoyancy driven rolls that make the undulating periodicity smaller as observed on the H-Si(100) surface. However, we could not observe such rolls at lower temperatures on the H-Si(100) surface as we did for the other two substrates, most likely due to the different reactivity of the three substrate surfaces. The "striped" films were easily observable at the back end of the substrate using a scan range of 100 nm for all surfaces, while at larger (1 μm) scales only H-Si(100) exhibited undulations. The lower bubbler temperature for appearance of the rolls on the amorphous oxide may be due to the isotropic nature of the native oxide, which allows the HTB molecules and reaction products of the CVD process to diffuse more easily than on a H-Si(100) surface. The observation of wavy films on native oxide with a bubbler temperature of 50°C is consistent with the largest RMS roughness at that temperature as shown in Figures 5 and 6. No obvious undulating patterns were observed at the other three temperatures.

Modeling and Discussion

Fluid behavior model

The gas flow in the CVD reactor may influence the extent of nonuniformity in thin film thickness and composition. The

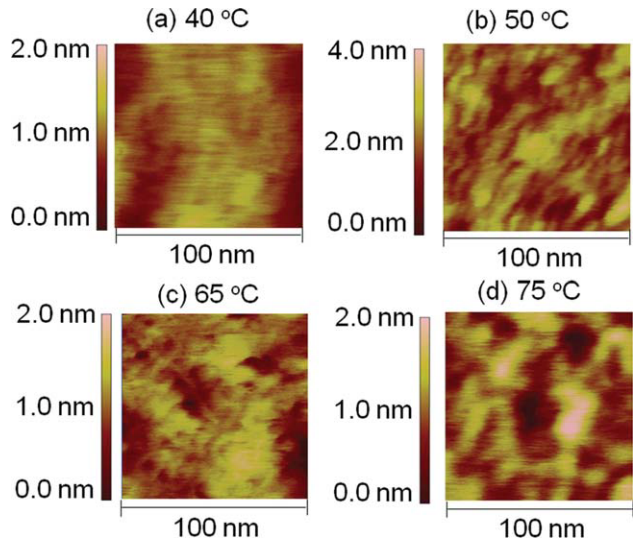

Figure 6. AFM images for films on native oxide at the back end of the substrate at $X = 3$ cm with a ST at 250°C with various bubbler temperatures: (a) 40, (b) 50, (c) 65, and (d) 75°C.

The larger roughness at 50°C required a larger scale. [Color figure can be viewed in the online issue, which is available at wileyonlinelibrary.com.]

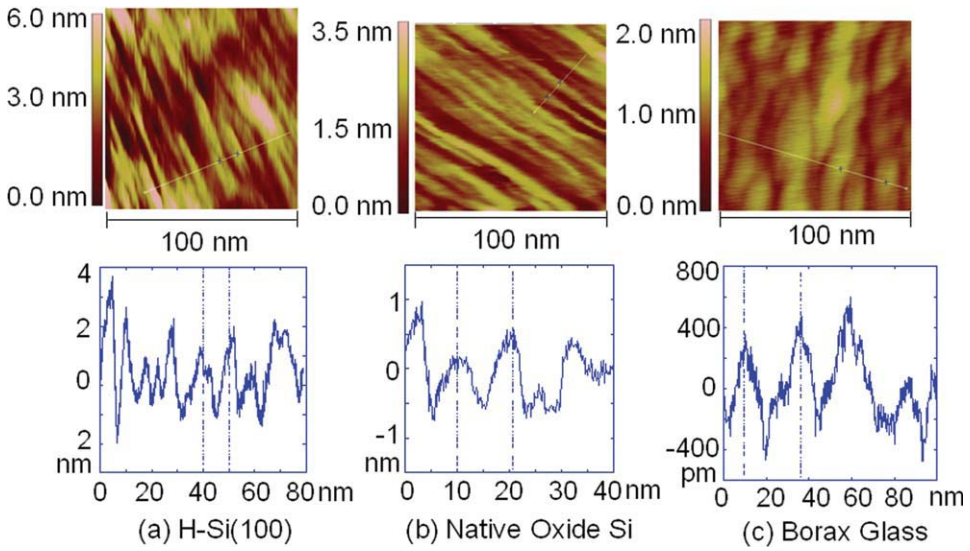

Figure 7. The upper row shows AFM images at X = 3 cm for 1 h HTB deposition with (from right to left): (a) 65°C bubbler temperature on 250°C hydrogen terminated Si(100) crystal, (b) 50°C bubbler temperature on 250°C native silicon oxide, and (c) 50°C bubbler temperature on 250°C Borax glass.

The lower row shows section measurements showing sampled periodicities: (a) 10, (b) 11, and (c) 25 nm. [Color figure can be viewed in the online issue, which is available at wileyonlinelibrary.com.]

fluid behavior is complex, depending on the geometry and operational settings (temperature, pressure, and flow rate). Vortices are normally undesirable for either film uniformity or interface abruptness.[13] The flow type is usually sensitive to several parametric numbers: Reynolds number Re, Grasholf number Gr, Raleigh number Ra, and Knudsen number Kn. At Re less than 2000, the flow is laminar. For laminar Poiseuille flow in a rectangular horizontal duct, Gr or Ra large enough to exceed a certain critical point can result in mixed convective flow.[7] The relation between Re and Ra is considered to influence the occurrence of longitudinal or transverse rolls.[15]

In the early 1980s, visual experiments were performed for liquid Poiseuille flow[14] and TiO_2 smoke in horizontal reactors with flow perpendicular to the susceptor.[15] The geometry of these reactors were designed with a hot substrate and cold wall. The flow was Rayleigh-Bénard natural convection in addition to a Poiseuille flow. The Rayleigh-Bénard case describes the formation of natural convection flow in a system with a large enough temperature difference between the top and bottom plates to overcome the viscosity and thermal diffusivity, when the Rayleigh number *Ra* (defined by Equation (1)) exceeds a certain critical value.

$$Ra = \frac{\alpha\beta g d^4}{kv} \tag{1}$$

where $\beta = \frac{dt}{dz} = \frac{\Delta T}{d}$, g is the acceleration due to gravity, α is the coefficient of thermal expansion, d is the depth of the chamber and k, v are the thermal diffusivity and kinematic viscosity respectively.

For this mesoscale horizontal flow reactor with top and bottom plates having a large temperature difference, mixed convection phenomena can possibly occur. To estimate the above characteristic fluid dynamic parameters, thermal properties of the precursor, HTB, were obtained using density functional theory (DFT) calculations with the Gaussian 03 software.[16] The DFT geometry optimizations and calculations of thermodynamic quantities were performed with the 6-31+G(d,p) basis set for the nonmetal atoms and the LanL2DZ large core relativistic effective core potential and associated basis set[17] for the Hf atom. The molecular diameter of the HTB molecule, d, was estimated to be 9.15 Å, and the calculated constant volume heat capacity C_v = 0.4551 kJ mol^{-1} K, gives a specific heat capacity of 0.9636 kJ kg^{-1} K^{-1}. With a molecular weight of 0.4722 kg/mol, the thermal conductivity coefficient k_T is calculated to be 0.03 W m^{-1} K^{-1} [given by Eq. (2)] and the dynamic viscosity η is about 1.25×10^{-5} Pa s [given by Eq. (3)] based on the rigid hard sphere theory for gases,[18] and is of the same order of magnitude as the viscosity estimated by using Hagen-Poiseuille equation.[19]

$$k = \frac{25}{32}\frac{\pi C_v}{N_A}\left(\frac{RT}{\pi m}\right)^{1/2}\frac{1}{\pi d^2} \tag{2}$$

$$\eta = \frac{2kM}{5C_v} \tag{3}$$

In the above equations R is the gas constant, T is the temperature, and m is the molecular weight. The flow is assumed as incompressible. The average flow rate of HTB is around 0.25 Pa-L/s, which corresponds to an average inlet velocity of 0.34 m/s in the 1/4″ 316 ss tube. Thus the Mach number is small enough to assume the steady state flow is incompressible.

With these values and a temperature difference of 100°C with a set point of 250°C at the top heating plate, the estimated characteristic parameters are summarized in Table 1. The temperature used in the estimation is 60°C, at 40.0 Pa. For incompressible flow, the coefficient of thermal expansion is assumed using air's thermal expansion coefficient $\alpha = 3 \times 10^{-3}$ K^{-1}. The characteristic length of the reactor is 4 mm. Since $Gr/Re^2 \sim 0.1$, any small fluctuation in the parameters may cause the ratio to be bigger than 1 so that the natural convection has to be taken into consideration.

Table 1. Estimated Fluid Mechanics Parameters for 60°C HTB at 0.3 Torr

Name	Definition	Value
Knudsen	$Kn = \frac{l}{L}, l = \frac{1}{\sqrt{2}\pi d^2 n}, n = \frac{pN_A}{RT}$	0.0075
Mach	$Ma = \frac{v}{c}$	0.0065
Prandtl	$\mathrm{Pr} = \frac{C_p \cdot \eta}{M \cdot k_T}$	0.41
Reynolds	$\mathrm{Re} = \frac{\rho \cdot v \cdot d}{\eta}$	0.83
Grashof	$Gr = \frac{Ra}{\mathrm{Pr}} = \frac{\rho^2 g \Delta T \alpha d^3}{\eta^2}$	0.07
Raleigh	$Ra = Gr \cdot \mathrm{Pr}$	0.03

The flow working volume is composed of two half-cut circular cones with radiuses R (8 cm) and r (4 cm), respectively, and an inverse trapezoid with matching sides on the diameter with the two half cones. The height d between the inlet and the substrate is 4 mm, and the length, L, of the flow path on the substrate is 45 mm, which gives a finite horizontal duct $L/d \sim 10$. Because of mixing of longitudinal rolls and transverse convection, the calculation has to be performed as a three-dimensional model.

The governing equations can be written as a set of Navier–Stokes (N–S) equations for continuity, momentum and energy balances. The velocities and pressure can be solved iteratively through implicit or explicit ways in the finite volume method, and then will give other transport scalars. For steady state incompressible flow, the nonconservative form of the N–S equations are:[4,7]

$$\nabla \cdot \mathbf{u} = 0 \tag{4}$$

$$\nabla \cdot \rho \mathbf{u}\mathbf{u} = -\nabla p + \nabla \left\{ \mu \left[\nabla \mathbf{u} + (\nabla \mathbf{u})^T - \frac{2}{3}(\nabla \mathbf{u}) \cdot \mathbf{I} \right] \right\} \tag{5}$$

$$\rho C_p \mathbf{u} \cdot \nabla T = \nabla_2 \cdot (k \nabla_2 T) + \sum_{i=1}^{s} \overline{H}_i \left[\left(\nabla \cdot \mathbf{J}_i - \sum_{j=1}^{g} v_{ji}^g R_j^g \right) \right] \tag{6}$$

where the $\mathbf{u}$ is the velocity vector, $\boldsymbol{I}$ is the unit tensor, and superscript T is the transpose of the tensor, H_i is the energy for reaction i, $\mathbf{J}_i$ is the molar flux, and v_{ii} is the stoichiometric coefficient. Dufour and Soret diffusion[20] for reactants and by-products are neglected here.

Even without complex flow patterns, the analysis of the deposition rate determining film uniformity and composition with real-operation parameters is a nontrivial task. The quantitative analysis of transverse dispersion in a particular flow has to be analyzed with precise calculations, which require careful setting of the parameters. Mixed convection may affect the thin film growth on the concentration of vapor supply and density of films. For a horizontal reactor with its substrate having a uniform temperature profile, an inert gas stream velocity at steady state was modeled. The characteristic velocity profile with 1.7 Pa-L/s flow rate is shown in the Supporting Information Figure S5 using a very fine mesh. The parabolic shape of the velocity is due to the viscosity. A nonslip assumption was made consistent with laminar flow.

With a temperature difference of about 100°C between the top heated plate and the bottom substrate at ST = 250°C, the Ra number suggests the possibility of roll formation in the gas phase flow, which is known as the Bénard thermal instability problem.[21] Instead of incorporating possible homogeneous and heterogeneous reactions for film growth, a simplified model with only a pure N_2 flow pattern was simulated.

Figure 8 shows the mixed convection predicted by the calculations and verified in the AFM images. The left column contains AFM images of the thin film surface at three locations along the axis on the native oxide substrate. The ST temperature was 250°C, the bubbler temperature was 50°C, and the deposition duration was 1 h. The middle and right columns are the CFD calculated flow behavior for 1.7 Pa-L/s N_2 in the isothermal flow cell with the top plate at 250°C, bottom substrate at 145°C, and the wall at 150°C. Mixed convection was observed. At the inlet and outlet positions, free convection occurs and forms a roll-type flow. Compared with the AFM image on the left, it can be seen that the flow pattern indeed influences the growth of the film by its

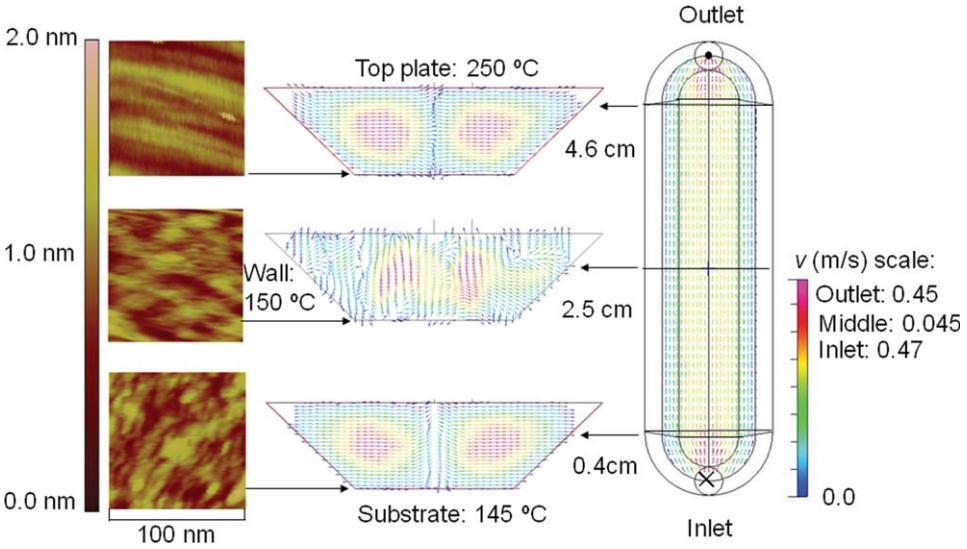

Figure 8. Mixed convection and film morphology at ST of 250°C on native oxide.

[Color figure can be viewed in the online issue, which is available at wileyonlinelibrary.com.]

morphology in addition to the growth rate as discussed above. An undulating type film surface was observed at the later part of the substrate. However, the exact location was difficult to control due to the instability of the flow and the scale of the meso-reactor. The inlet and outlet flow patterns are similar but a little different due to different flow directions. Only at the backend of the substrate was the wavy surface observed experimentally, as the first AFM image shown in Figure 8. One possibility may be due to a more stable roll at the end of the meso scale flow reactor. Although the inlet and outlet flow patterns are predicted to be similar at steady state, there could be more perturbations and instabilities at the inlet than at the outlet where the pressure is reduced due to reactions of the HTB on the substrate. This is the first time that such a prediction from this type of flow modeling has been verified by measurements of the morphology of the thin film. Further study of this phenomenon using longer reactors can provide more quantitative measurements of the relationship between the flow and the periodicity of the rolls.

The formation of roll type flow may be the reason why the observed roughness and thickness changes are observed. The enhanced roughness of the HfO_2 thin film on the native oxide at the 50°C bubbler temperature may correspond to the onset of stable rolls. Although the roll type flow would be easier to form when the vapor pressure increases with an increase of bubbler temperature, due to a larger Grashof number, the velocity also increases which in turn increases the critical Rayleigh number to form the transversal rolls.[15] In other words, rolls may form more easily at this vapor pressure than at lower vapor pressures, but the velocity must remain low enough to not increase the critical Rayleigh number. However, further study is needed to verify this theory. In addition, the rolls increased with residence time and may enhance the diffusivity at the microscopic level. When diffusivity is faster than advection, the concentration field downstream can be bigger than upstream, which may explain the thickness increase downstream as discussed above.

Conclusions

HfO_2 thin films were grown in a Horizon™ flow cell to optimize operational parameters for a better film uniformity. The depletion problem common in horizontal reactors was found to be tunable with different precursor supply flow rates. When the top heating plate temperature was set to be 250°C, there was a temperature difference of 100°C between the top heated plate and the bottom substrate, which caused mixed convection for the flow in the cell with a bubbler temperature between 50 and 75°C. The roll type flow influenced thin film growth and was confirmed by AFM. However, the periodicity of the rolls cannot be controlled very well by flux or other experimental parameters at this time and further study of this phenomenon is needed.

Acknowledgments

The authors would like to thank Dr. Elizabeth Moore, William Kimes, James Maslar of the National Institute of Standards and Technology for the computational fluid dynamics calculations, Dr. Muhammad Ali Rob Sharif and Dr. Peter E. Clark at The University of Alabama for helpful discussions about complex flow and Dr. Susan Berets in Harrick Scientific, for providing the detailed flow cell dimensions. This work was supported in part by NSF CAREER award #0239213 to T.K. This work was supported in part by the Chemical Sciences, Geosciences and Biosciences Division, Office of Basic Energy Sciences, U.S. Department of Energy (DOE) under grant no. DE-FG02-03ER15481 (catalysis center program) and by the National Science Foundation (CTS-0608896), through the NIRT program. DAD also thanks the Robert Ramsay Chair Fund of The University of Alabama for support.

Literature Cited

1. Smith DL. *Thin Film Deposition Principles & Practice*. New York: McGraw-Hill, Inc., 1995.
2. Privorotskaya NL, King WP. Silicon microcantilever hotplates with high temperature uniformity. *Sens Actuators A Phys*. 2008;152:160–167.
3. Kleijn CR. A Mathematical model of the hydrodynamics and gas-phase reactions in silicon LPCVD in a single-wafer reactor. *J Electrochem Soc*. 1991;138:2191–2200.
4. Jensen KF. Flow phenomena in chemical vapor deposition of thin films. *Annu RevFluid Mech*. 1991;23:197–232.
5. Jensen KF. Micro-reaction engineering applications of reaction engineering to processing of electronic and photonic materials. *Chem Eng Sci*. 1987;42:923–958.
6. Jensen KF. Transport phenomena and chemical reaction issues in OMVPE of compound semiconductors. *J Cryst Growth*. 1989;98:148–166.
7. Moffat H, Jensen KF. Complex flow phenomena in MOCVD reactors: I. Horizontal reactors. *J Cryst Growth*. 1986;77:108–119.
8. Frank MM, Sayan S, Dörmann, Emge TJ, Wielunski LS, Garfunkel E, Chabal YJ. Hafnium oxide gate dielectrics grown from an alkoxide precursor:structure and defects. *Mater Sci Eng B*. 2004;109:6–10.
9. Li K, Dubey S, Bhandari HB, Hu Z, Turner CH, Klein TM. *In situ* attenuated total reflectance Fourier transform infrared spectroscopy of hafnium (IV) *tert* butoxide adsorption onto hydrogen terminated Si (100) and Si (111). *J Vac Sci Tech A*. 2007;25:1389–1394.
10. Quiram DJ, Jensen KF, Schmidt MA, Mills PL, Ryley JF, Wetzel MD, Kraus DJ. Integrated microreactor system for gas-phase catalytic reactions. 3. Microreactor system design and system automation. *Ind Eng Chem Res*. 2007;46:8319–8335.
11. Mehrotra RC, Bradley DC, Rothwell IP, Singh A. *Alkoxo and Aryloxo Derivatives of Metals*, Revised ed. San Diego, CA: Academic Press, 2001.
12. Cameron MA, George SM. ZrO_2 film growth by chemical vapor deposition using zirconium tetra-*tert*-butoxide. *Thin Solid Films*. 1999;348:90–98.
13. Patnaik S, Brown RA. Hydrodynamic dispersion in rotating-disk omvpe reactors: numerical simulation and experimental measurements. *J Crystal Growth*. 1989;96:153–174.
14. Luijkx JM, Platten JK, Legros JC. On the existence of thermoconvective rolls, transverse to a superimposed mean Poiseuille flow. *Int J Heat Mass Transf*. 1981;24:1287–1291.
15. Setyawan H, Shimada M, Ohtsuka K, Okuyama K. Visualization and numerical simulation of fine particle transport in a low-pressure parallel plate chemical vapor deposition reactor. *Chem Eng Sci*. 2002;57:497–506.
16. Gaussian 03, Revision E.01, Frisch MJ, Trucks GW, Schlegel HB, Scuseria GE, Robb MA, Cheeseman JR, Montgomery, Jr. JA, Vreven T, Kudin KN, Burant JC, Millam JM, Iyengar SS, Tomasi J, Barone V, Mennucci B, Cossi M, Scalmani G, Rega N, Petersson GA, Nakatsuji H, Hada M, Ehara M, Toyota K, Fukuda R, Hasegawa J, Ishida M, Nakajima T, Honda Y, Kitao O, Nakai H, Klene M, Li X, Knox JE, Hratchian HP, Cross JB, Bakken V, Adamo C.; Jaramillo J, Gomperts R, Stratmann RE, Yazyev O, Austin AJ, Cammi R, Pomelli C, Ochterski JW, Ayala PY, Morokuma K, Voth GA, Salvador P, Dannenberg JJ, Zakrzewski VG, Dapprich S, Daniels AD, Strain MC, Farkas O, Malick DK, Rabuck AD,

Raghavachari K, Foresman JB, Ortiz JV, Cui Q, Baboul AG, Clifford S, Cioslowski J, Stefanov BB, Liu G, Liashenko A, Piskorz P, Komaromi I, Martin RL, Fox DJ, Keith T, Al-Laham MA, Peng CY, Nanayakkara A, Challacombe M, Gill PMW, Johnson B, Chen W, Wong MW, Gonzalez C, Pople JA, Gaussian, Inc., Wallingford CT, 2004.
17. Wadt WR, Hay PJ. Ab inito effective core potentials for molecular calculations. Potentials for main group elements Na to Bi. *J Chem Phys*. 1985;82:284–298.
18. Clyde RM. *Physical Chemistry*, New York: McGraw-Hill, 1988: 27–28.
19. Hagenbach EP. Annalen der Physik u. *Chemie*. 1860;108:385–426.
20. Grew KE, Ibbs TL. *Thermal Diffusion in Gases*. Cambridge U.K: Cambridge University Press, 1952.
21. Kundu PK, Cohen IM. *Fluid Mechanics*, 2nd ed. San Diego, CA: Academic Press, 2002.

Manuscript received Sep. 25, 2010, and revision received Nov. 18, 2010.